Spectral Beam Combining of Fiber Lasers by Using Reflecting Volume Bragg Gratings *

Tai-Dou Zhou(周泰斗), Xiao-Bao Liang(梁小宝), Chao Li(李超), Lei Zhao(赵磊), Jian-Jun Wang(王建军), Feng Jing(景峰)**

Laser Fusion Research Center, China Academy of Engineering Physics (CAEP), Mianyang 621900

(Received 8 September 2016)

By employing three reflecting volume Bragg gratings, a near-infrared 4-channel spectral-beam-combining system is demonstrated to present 720 W combined power with a combining efficiency of 94.7%. The combined laser beam is near-diffraction-limited with a beam factor $M^2 \sim 1.54$. During this 4-channel beam-combining process, no special active cooling measures are used to evaluate the volume Bragg gratings as combining elements are under the higher power laser operation. Thermal expansion and period distortion are verified in a 2 kW 2-channel beam-combining process, and the heat issue in the transmission case is found to be more remarkable than that in the diffraction case. Transmitted and diffracted beams experience wave-front aberrations with different degrees, thus leading to distinct beam deterioration.

PACS: 42.55.Wd, 42.40.Pa, 42.40.Eq DOI: 10.1088/0256-307X/33/12/124205

High power fiber lasers[1] with good beam quality are needed for a variety of applications such as in scientific research, national defense and medical surgery. However, to scale up the output power of a single amplifier to a higher power level is a problem confronting many challenges such as nonlinear effects,[2,3] thermal loading,[4] fiber damage,[5] pump brightness[6] as well as mode instability,[7–9] which limit the final laser output power. To bypass these fundamental restrictions, combining laser beams have been proposed to be an alternative approach for power and brightness scaling.[10] Currently, there are two brightness scaling approaches: coherent beam combining (CBC) and spectral beam combining (SBC),[10,11] which have been under intensive study over the past decade. CBC is very attractive for its beam intensity enhancement while it requires a very complex optical system and accurate phase-control measures. On the contrary, SBC is an incoherent technique to simply combine different laser beams together without the need for fine phase control and therefore allow for a stable and robust system.[12] Further thanks to excellent thermal stability, mechanical strengths and high laser damage threshold, volume Bragg gratings (VBGs) have been used as combining elements in high-power SBC regime lately, i.e., the VBG-SBC system.[13]

In a VBG-SBC system, there must be interaction between laser radiation and VBG matrix. The reflectivity and stability of these VBGs would be largely affected by the temperature profile, which depends on the incident laser beam profile, the thermal conductivity and the heat exchanging-rate between the VBGs and the surroundings. High power diffraction-limited fiber lasers always have a quasi-Gaussian intensity distribution, which leads to a higher temperature in the center while a lower temperature at the edge and hence lead to thermal expansion and period distortion in VBGs, resulting in non-uniform angular diffractions and thermal-induced wave-front aberrations.

In this study, by employing three reflecting VBGs, a near-infrared 4-channel spectral-beam-combining system is demonstrated to present 720 W combined power with a combining efficiency of 94.7%. The combined laser beam is near-diffraction-limited with a beam factor $M^2 \sim 1.54$.

To obtain efficient SBC laser output, the performance of VBGs and other optical units should be tested under high power radiation conditions. Thermal behavior of VBGs is investigated experimentally. Due to intrinsic material absorption, Gaussian laser beams can lead to thermal expansion and period distortion in VBGs, resulting in different thermal induced wave-front distortions for both transmitted and diffracted beams, i.e., degradation of the finally combined beam quality. It is important to note that no active cooling measures were taken during these VBG-SBC processes.

Figure 1 illustrates the schematic diagram and experimental setup of the 4-channel VBG-SBC system. Mounted on an optical table, this VBG-SBC system consists of three parts: laser sources, a combining part and a measurement part.

(i) The laser sources comprise four home-made high power narrow-line-width Yb-doped fiber lasers, and each fiber laser can present a maximum output power of ∼1.5 kW with a near-diffraction-limited beam $M^2 < 1.5$. For safety and to avoid ther-

*Supported by the National Natural Science Foundation of China under Grant Nos 11474257 and 61605183.
**Corresponding author. Email: jingfeng09@sina.cn
© 2016 Chinese Physical Society and IOP Publishing Ltd

mal damage without cooling measures, each fiber laser was set to ∼190 W with $M^2 < 1.2$. The central wavelengths of these four fiber lasers are set at 1055.3 nm, 1057.4 nm, 1059.4 nm and 1062.5 nm, and the corresponding spectral widths are 0.1 nm, 0.08 nm, 0.106 nm and 0.101 nm, respectively. Each fiber laser beam is properly collimated by 6 mm in diameter, ready for the following combining procedure.

(ii) In the combining part, three reflecting Bragg gratings (RBGs) are arranged in a cascaded geometry. Each RBG is with diffraction efficiency >97%, spectral selectivity of ∼0.75 nm (FWHM), thickness of 2.6 mm and input-angle of ∼6° in air at 1053 nm. Reflecting mirrors are used to steer beams towards RBGs. By adjusting the distance between mirrors and RBGs and the angles of RBGs, incident laser beams can match the corresponding RBGs. The chosen laser beam with the right wavelength can be properly diffracted while the other laser beams with offset wavelengths are transmitted. The transmitted and diffracted beams finally overlap in the near- and far-field and a resulting combined collinear-beam is achieved.

(iii) A wedge prism is used to separate a fraction of the combined beam into a measurement part, recording laser spectrum and measuring beam quality in time.

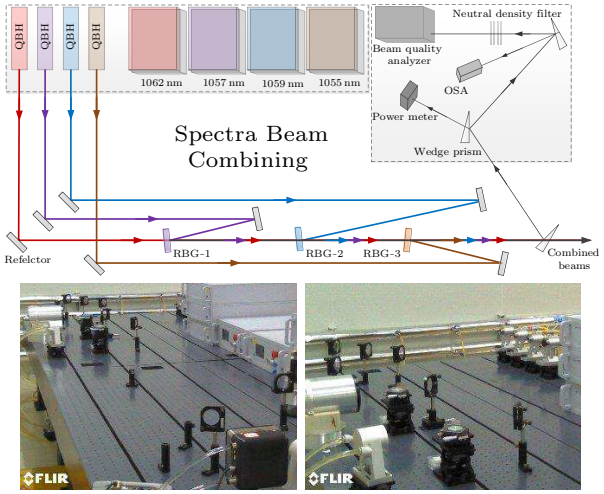

Fig. 1. The 4-channel VBG-SBC system.

A red laser-diode bar with a single-mode fiber pigtail was used as the index laser to align this designed VBG-SBC system, which was coupled into the home-made 1062.5 nm laser by a (2+1)×1 combiner in the main oscillator. Thus the index laser and the 1062.5 nm laser overlapped to define the output axis. By using a charge-coupled device (CCD) in a beam quality analyzer (M2-200 s, Spiricon), the intensity profile in the near- and far-field can be observed, judging the beam overlap ratio. The 1062.5-nm-beam transmitted through all the VBGs (RBG-1 to RBG-3) as shown by the red line and arrow in Fig. 1. The other wavelength-laser beams are aligned sequentially, starting with one that is closer to the index laser and ending with one that is closer to the output. By angle-tuning the RBG and adjusting the distance from the mirror to the corresponding RBG, the transmitted and diffracted beams are superposed in the near- and far-field according to the overlapped intensity profile on the CCD. This procedure is repeated to align the next channel, and the alignment is performed under low power conditions. After all the channels are aligned properly, the channel power was increased to ∼190 W, resulting in a combined output power of 720 W. It should be noted that perfect alignment is implemented at low power, and re-alignment should be necessary when increasing the input power. This can be carried out by means of angle-tuning or the thermal tuning technique.[14] During this experiment, we angle-tuned the RBGs to make the combined beams re-collinear. The combining efficiency is measured at about 97% for low power level at 100 W while reduced to 94.7% for high power level at 720 W, the reason for the small decline of efficiency should be attributed to spectrum broadening and cross loss. RBGs used in this experiment have a spectral selectivity of ∼0.75 nm (HWFZ) and peak efficiency > 97% as shown in Fig. 2(b). The cross loss results from the product of local max in the efficiency curve and the transmitted beam. To obtain higher overall combining efficiency, the 3rd or even higher-order minimum in the diffraction efficiency curve for the transmitted beams has to be found. Figure 2(a) depicts the measured spectrum for all the channels covering a spectral range from 1055 nm to 1063 nm.

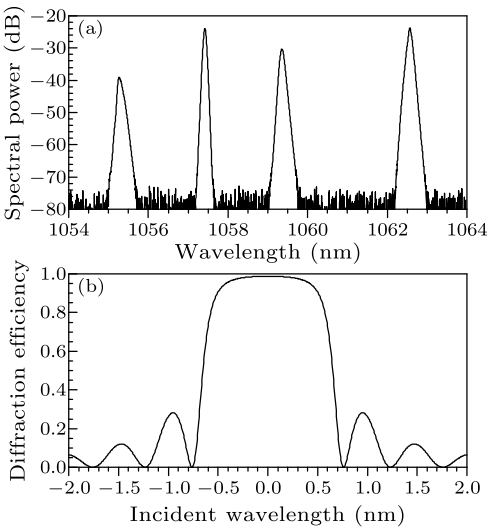

Fig. 2. (a) The measured spectrum of the combined beam. (b) The efficiency curve and ∼2 nm selected channel spacing.

The combined beam quality is measured by a beam quality analyzer (Spiricon, M^2-200 s) by focusing beam arrays through a lens. Along the direction

of focused beams, a CCD is used to scan the beam intensity profile in multiple planes and to calculate the beam waist size by the second moment definition. The far-field divergence angle is measured by fitting multiple beam widths to a hyperbolic equation curve. The beam quality factor M^2 is defined as the measured far-field divergence angle divided by the far-field divergence angle of an ideal Gaussian beam with an equivalent beam waist size. At the end, the combined beam has a rising M^2 as the input channel power increases as depicted in the right scale of Fig. 3(a). Here M^2 is ∼1.2 for low power of 100 W while $M^2 = 1.54$ for 720 W as inserted in Fig. 3(a) showing its near-field beam profile. Moreover, the peak temperature of RBG-3 increases with the input power as illustrated in Fig. 3(b). At 720 W, the peak temperature is raised by 27 K.

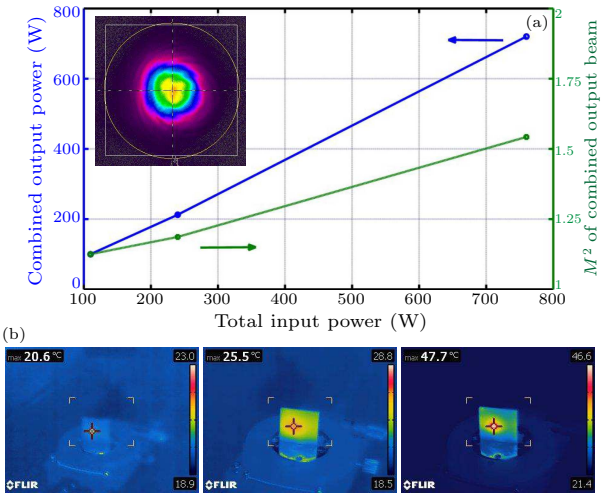

Fig. 3. (a) The combined output power and beam quality versus the total input power. The inset shows the near field at 720 W output. (b) The hot image of RBG-3 in a low-middle-high power situation.

It is worth noting that RBGs are spectrally selective optical elements and they are not angularly dispersive,[15–17] and the interaction with spectral width will not deteriorate M^2. For our home-made fiber lasers, output of each channel is narrow-linewidth and has a power-independent M^2 value of ∼1.2 up to 190 W. Therefore, the deterioration of combined beam quality is possibly related to the thermal issue of the RBGs during the combining process. Even though RBGs have a low while finite absorption coefficient, this thermal absorption of near-Gaussian laser radiation will cause a remarkable increase of the non-uniform temperature, resulting in higher temperature in the central while lower in the edge to form a thermal gradient, and results in non-uniform thermal expansion and non-uniform grating period distortion.

To further investigate thermal issues and other possible factors leading to beam quality degradation, we increased the incident power onto the VBGs. In a 2-channel SBC system, 2 kW total input power was delivered to RBG-1, as illustrated in Fig. 4, the first 1062.5-nm-beam was transmitted (red line) while the second 1057.4-nm-beam was diffracted (purple line). The maximum powers of the transmitted and diffracted beam are set as 1100 W and 900 W, respectively. Both beams propagated in the same space and in the same direction, resulting in an overlapped output with 1620 W combined output. Combined efficiency is ∼81%, mainly due to the non-uniform grating period distortion, since fiber lasers are narrow line-width outputs. As a result of higher power within the RBGs, heavier thermal issues occur, and the combined beam quality becomes worse with $M^2 = 3.75$.

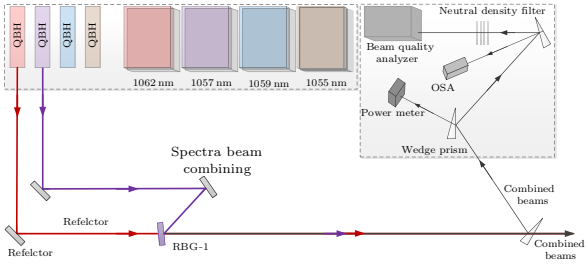

Fig. 4. Schematic configuration of the 2-channel SBC setup.

For SBC, the combined beam quality is an important indicator. Combining elements like VBGs rest mainly on the beam conservation. Generally speaking, for the spatial combining technique, such as VBG-SBCs, the combined beam quality is determined by the uniformity of spatial beam properties.[18] Such properties can be beam size, beam overlap ratio and wave-front characteristics like convergence and divergence, respectively. Variations of these properties among the single channel will lead to a degradation of the combined beam quality.

In the 2-channel SBC, each fiber laser has good beam quality with $M^2 < 1.5$ in the whole power range and the initial beam size is set as 6 mm (FWe^{-2}M). Therefore, the beam size difference between sub-beams occurs only during the combining process: (1) RBGs are spectrally selective optical elements and they are not angularly dispersive, and bandwidth increase does not lead to the increase of the beam size. (2) The diffracted beam and transmitted beam propagate with different distances in space and after RBGs there will be beam size difference, which is too small and is not the reason for the observed deterioration of M^2. Further, the decline of beam overlap ratio between sub-beams will also affect beam quality. In this experiment, perfect alignment is implemented in the low power situation, and non-uniform period distortion will cause a decline of the beam overlap ratio when increasing the power. To exclude this effect, proper angle tuning is implemented to make the sub-beams re-collinear. At the end, the significant deteri-

oration of combined beam quality is rather related to the wave-front characteristics of sub-beams caused by the 'hot' RBGs.

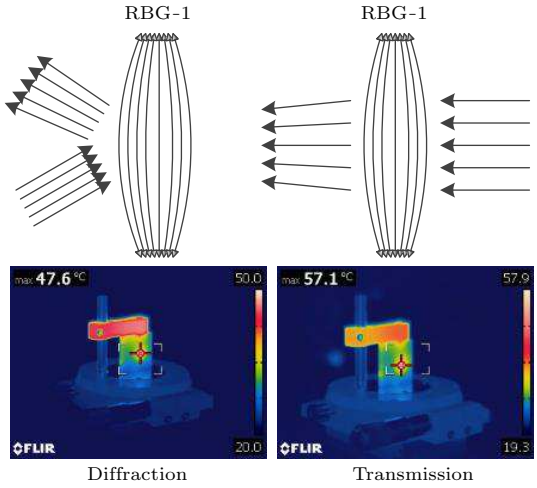

Fig. 5. Schematic diagram of wave-front aberrations and hot-image of RBG-1.

Figure 5 depicts the schematic diagram of the wave-front aberrations of sub-beams. To analyze wave-front characteristics, we measured the diffraction of 1057.4 nm laser and the transmission of 1062.5 nm laser on RBG-1, respectively. In both cases, we can observe a temperature increase of the RBG-1 when increasing the input power. For the photo-thermo-refractive glass, it is shown that the absorption coefficient is as low as $2\times10^{-4}\,\mathrm{cm}^{-1}$, which is closely related to the intrinsic absorption coefficient and the grating thickness. For the case of diffraction, it is shown that 90% of the laser power only encounters the first quarter of the RBG,[19] while for the case of transmission, power is distributed in the whole volume of the grating. Therefore, compared with diffraction, the transmission case contributes more heat to RBG-1, as can be seen in Fig. 5.

The RBGs are made with PTR glass. The refractive index rarely varies with temperature, typically less than 10^{-6}/K, while the thermal expansion is largely determined by an expansion coefficient of about 10^{-5}/K. In the transmission case, thermal absorption of RBG-1 causes a change in refractive index modulation and also bulges on both surfaces, acting as a thermal lens leading to a convergence of the transmitted beam. However, the reflected beam from the other side is only influenced by the surface bulge and causes a divergence of the diffracted beam as shown in Fig. 5. To confirm this, we experimentally measured the focus shift in both transmission and reflection cases.

Figure 6(a) depicts that with the increase of the input power, the focus shift in the transmission case is significant. While in the diffraction case, the focus shift is small (not exceeding 10 mm). In a low power situation for the diffraction case, the focus shift increases with the input power. However, the focus shift decreases when increasing the input power to 0.9 kW, indicating the existence of the thermal induced non-uniform period distortion. Period distortion of the RBG causes angular properties distortion of VBG, which will in-turn lead to a convergence of the diffracted beam. Figures 6(b) and 6(c) depict the spectrum of the input diffracted beam at 0.9 kW and the transmitted beam at 1.1 kW, respectively.

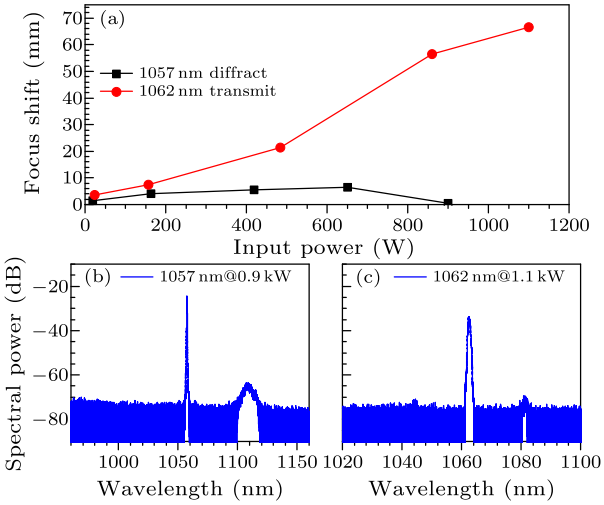

Fig. 6. (a) The shift of focus position of tested single transmitted and diffracted beam. Spectrum of (b) 1057 nm diffracted beam at 0.9 kW, and (c) 1062 nm transmitted beam at 1.1 kW.

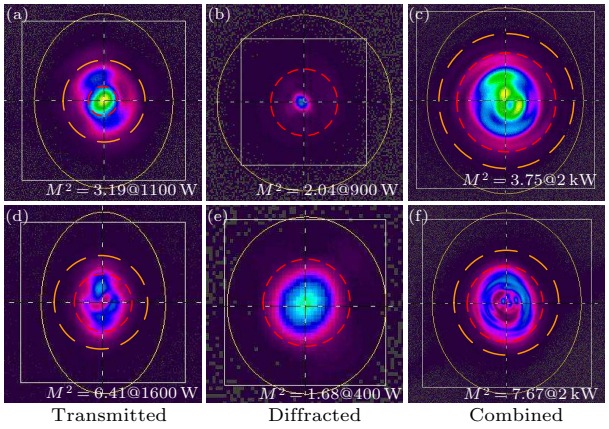

Fig. 7. Measured M^2 and transversal beam profiles for (a) and (d) transmitted, (b) and (e) diffracted, (c) and (f) combined beam at different maximum powers.

The measured M^2 of the diffracted beam is increased to 2.04 at 1.1 kW, and the measured M^2 of the transmitted beam is 3.19 at 0.9 kW. Figure 7 illustrates M^2 and the transversal beam profiles at the focal plane for the transmitted, diffracted and the resulting combined beam. For the transmitted beam shown in Fig. 7(a), one can discover a distorted beam profile, since the thermal lens will only affect the concentration degree of the focal spot. The distorted spot is related to the thermal induced period distortion, be-

cause the non-uniform distortion of the grating period will lead to the degradation of the diffraction characteristics and the angular selectivity. For the diffracted beam in Fig. 7(b), less input power and less heat contribute to the RBG-1 compared with the transmitted beam, thus the deterioration of the transversal profile is not significant. Also, the stretch in transverse direction is not obvious, indicating that the RBGs are spatial-dispersion-free. The transmitted beam and diffracted beam have different wave-front aberrations. Once they are combined, more heat on RBG-1 will intensify the thermal expansion and non-uniform grating period distortion. Consequently, the combined beam shows a distorted beam profile and the beam quality becomes worse with $M^2 = 3.75$ as illustrated in Fig. 7(c).

Keeping the total input power of 2 kW unchanged, we change the input power ratio between the transmitted and diffracted beam, the measured M^2 of the diffracted beam is 1.68 at ∼400 W, while the beam quality of the transmitted beam is increased to 6.41 at ∼1600 W. The transmitted beam has the ability to produce up to 2 kW power with $M^2 \leq 1.8$. Figures 7(d)–7(f) illustrate M^2 and the transversal beam profiles for the transmitted, diffracted and the resulting combined beam. For the transmitted beam, RBG-1 encounters a dramatic expansion and non-uniform period distortion due to more absorption, resulting in worse beam quality compared with Fig. 7(a). However, the diffracted beam has a good $M^2 = 1.68$ and the focal spot is near-Gaussian intensity distributed. The power of the diffracted beam is only 400 W and the thermal effect within RBG-1 is not significant, as mentioned in the above diffraction case. Once the transmitted and diffracted beams are combined, the thermal effect becomes more serious, the combined beam quality is degraded to $M^2 = 7.67$ and the transversal beam profile of the focal spot shows a significant distortion, as illustrated in Fig. 7(f).

In conclusion, by employing three reflecting VBGs, a near-infrared 4-channel spectral-beam-combining system is demonstrated to present 720 W combined power with a combining efficiency of 94.7%. The combined laser beam is near-diffraction-limited with a beam factor $M^2 \sim 1.54$. VBGs have the potential to maintain a good beam quality for the spectrum beam combining system. Research is also focused on the thermal issue and the results indicate that thermal-induced wave-front distortions of the non-combined sub-beams lead to a deterioration of beam quality. Degradation of M^2 should be mainly attributed to the transmitted sub-beams. Thermal problems can be easier to mitigate if less power needs to be absorbed. By further reducing the absorption coefficient, VBGs used as combining elements could demonstrate great advantages in the SBC system. Other methods like a proper cooling system and beam shaping optics will contribute to overcoming these negative effects mentioned above.

All the results and the corresponding copyrights belong to the Laser Fusion Research Center, at China's Academy of Engineering Physics. We also express appreciation for the use of the equipment from the Optics Laboratory.

References

[1] Richardson D J, Nilsson J and Clarkson W A 2010 *J. Opt. Soc. Am.* B **27** B63
[2] Hu M, Yang Y F, Zheng Y et al 2016 *Chin. Phys. Lett.* **33** 044208
[3] Li L, Pang L H, Zhou Z G et al 2015 *Chin. Phys. Lett.* **32** 054201
[4] Ke W W, Wang X J, Bao X F et al 2013 *Opt. Express* **21** 14272
[5] Sun J Y, Xiao Q R, Li D et al 2016 *Chin. Phys.* B **25** 014204
[6] Chen X, Xiao Q R, Jin G Y et al 2015 *Chin. Phys.* B **24** 064208
[7] Smith A V and Smith J J 2011 *Opt. Express* **19** 10180
[8] Jauregui C, Eidam T, Limpert J and Tünnermann A 2011 *Opt. Express* **19** 3258
[9] Eidam T, Wirth C, Jauregui C et al 2011 *Opt. Express* **19** 13218
[10] Fan Y Y, He B, Zhou J et al 2011 *Opt. Express* **19** 15162
[11] Fan T Y 2005 *IEEE J. Sel. Top. Quantum Electron.* **11** 567
[12] Bochove E J 2002 *IEEE J. Quantum Electron.* **38** 432
[13] Sevian A, Andrusyak O, Ciapurin I et al 2008 *Opt. Lett.* **33** 384
[14] Drachenberg D R, Andrusyak O, Venus G B et al 2013 *Appl. Opt.* **52** 7233
[15] Drachenberg D R, Divliansky I, Smirnov V et al 2011 *Proc. SPIE* **7914** 79141F
[16] Andrusyak O, Smirnov V, Venus G et al 2009 *Opt. Commun.* **282** 2560
[17] Drachenberg D R, Andrusyak O, Venus G B et al 2014 *Appl. Opt.* **53** 1242
[18] Schmidt O, Wirth C, Nodop D et al 2009 *Opt. Express* **17** 22974
[19] Ott D, Divliansky I, Anderson B et al 2013 *Opt. Express* **21** 29620